

Analysis of flow through dam foundation by FEM and ANN models Case study: Shahid Abbaspour Dam

Mehrdad Shahrbanouzadeh^{*}, Gholam Abbas Barani^a and Saeed Shojaee^c

Department of Civil Engineering, Shahid Bahonar University of Kerman, P.B. 76169133, Kerman, Iran

(Received February 12, 2014, Revised April 05, 2015, Accepted May 21, 2015)

Abstract. Three-dimensional simulation of flow through dam foundation is performed using finite element (Seep3D model) and artificial neural network (ANN) models. The governing and discretized equation for seepage is obtained using the Galerkin method in heterogeneous and anisotropic porous media. The ANN is a feedforward four layer network employing the sigmoid function as an activator and the back-propagation algorithm for the network learning, using the water level elevations of the upstream and downstream of the dam, as input variables and the piezometric heads as the target outputs. The obtained results are compared with the piezometric data of Shahid Abbaspour's Dam. Both calculated data show a good agreement with available measurements that demonstrate the effectiveness and accuracy of proposed methods.

Keywords: seepage; dam foundation; finite element method; neural network; Seep3D model

1. Introduction

Seepage through dam foundation and the related piezometric pressures have been prompted more attention to the studies of dam construction projects. Different methods exist for analysis of seepage through earth dams and their foundations. Seepage paths have been predicted by both physical and mathematical models. Several numerical models are available for simulating water movement through saturated porous media (Rubin 1968, Cooley 1971, Krikland *et al.* 1992). Li *et al.* (1997) presented a numerical model based on the boundary element method, which simulates 2D groundwater flow with free and moving boundary conditions. This model is limited to a fully saturated and homogeneous domain (Li *et al.* 1997). Ataie-Ashtiani *et al.* (1999) performed a numerical and experimental study of seepage through unconfined aquifers with a periodic boundary condition. Panthulu *et al.* (2001) used an electrical resistivity method to delineate zones favorable to seepage and a selfpotential method to delineate seepage paths for two Saddle dams of the Som-Kamla-Amba project in Rajasthan, India. Turkmen *et al.* (2002) drilled boreholes and used dye trace tests to identify the seepage paths through the rock-fill Kalecik dam in Turkey.

^{*}Corresponding author, Ph.D. Student, E-mail: m.shahrbanouzadeh@eng.uk.ac.ir

^a Professor, E-mail: gab@mail.uk.ac.ir

^b Associate Professor, E-mail: Saeed.Shojaee@mail.uk.ac.ir

Honjo *et al.* (1995) used a finite element method (FEM) based on an invariant mesh technique to analyze of seepage through the saturated-unsaturated zone in the Tarbela dam in Pakistan. They analyzed various stages of reservoir filling and depletion and different conditions of reservoir sedimentation. Tien-Kuen (1996) investigated the stability of an earth dam under steady state seepage by FEM. Xu *et al.* (2003) designed a hydraulically optimal earth-dam cross section. Money (2006) compared the results of Seep/w and Seep3D software programs developed by Geo-Slope International. The project analyzed is a proposed excavation near the landside toe of the Sacramento River levee in Sacramento, California. Chang *et al.* (2010) used a mathematical model developed for analyzing of two-zone unconfined aquifer system and the associated solution for CHTs (constant-head test) at partially penetrating wells under transient state. Arun and Reddi (2011) obtained Closed-form theoretical solutions for steady seepage below a horizontal impervious apron with equal end cutoffs using Schwarz-Christoffel transformation. The resulting implicit equations involving elliptic integrals are used to obtain various seepage characteristics in no dimensional floor-profile ratios.

Artificial neural networks are mathematical modeling tools and computing systems that are especially helpful in the field of prediction and forecasting in complex settings. These computing systems are made up of a number of simple and highly interconnected processing elements that process information by their dynamic state response to external inputs (Caudill and Butler 1987). Mathematically, an artificial neural network can be treated as a universal approximator which has an ability to learn from examples without the need of explicit physics (ASCE Task Committee 2000, Tayfur *et al.* 2005). That is given an input it produces an output, without revealing the physics of the process (Rajurkar *et al.* 2002). ANNs have been recently employed for the solution of many hydraulic, hydrologic, and water resources problems such as rainfall runoff (Tokar and Johnson 1999, Rajurkar *et al.* 2004), sediment transport (Jain and Reddi 2001, Tayfur 2002, Nagy *et al.* 2002), solute transport (Aziz and Wong 1992), estimation of scour downstream of a ski-jump bucket (Azamathulla *et al.* 2005), estimation of scour below spillways (Azamathulla *et al.* 2006, 2008), prediction of scour below submerged pipeline crossing a river (Azamathulla and Zakaria 2011) and model tree approach for estimation of critical submergence for horizontal intakes in open channel flows (Ayoubloo *et al.* 2011). In this study both developed models of FEM and ANN were applied to predict seepage through foundation of Shahid Abbaspour Dam in Iran. The water levels at the upstream and downstream of the dam were used as input variables and those of the piezometers as the target outputs in the artificial neural network model. The Piezometer data since 1-19-1992 to 2-15-2002 have been used for monitoring of seepage and their pressure heads and the model results were compared with these piezometric data.

2. Governing equation

Fundamental to the formulation of a general seepage analysis is an understanding of the relationship between pore-water pressure and volumetric water content. As water flow through soil, certain amounts of water are stored or retained within the soil structure. The amount of water stored or retained is a function of the pore-water pressure and the characteristics of the soil structure. For a seepage analysis, it is convenient to specify the stored portion of the water flow as a ratio of the total volume. This ratio is known as the volumetric water content. In equation form

$$\theta = \frac{V_w}{V} \quad (1)$$

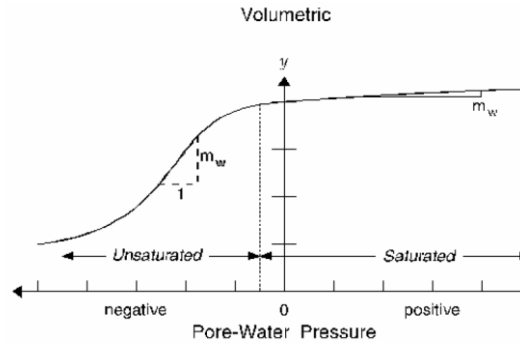


Fig. 1 General form of volumetric water content function

Where θ is volumetric water content, V_w is volume of water and V is total volume. The volumetric water content θ is dependent on the pore-water pressure. The Fig. 1 illustrates this relationship, which is also known as the soil-water characteristic function (Fredlund and Rahardjo 1993).

The flow of water through a soil mass can be described using Darcy’s law

$$v = ki \tag{2}$$

Where v is the Darcian velocity, i is potential gradient, and k is coefficient of permeability. Darcy’s Law was originally derived for saturated soil, but later research has shown that it can also be applied to the flow of water through unsaturated soil (Childs and Collins-George 1950). The only difference is that under conditions of unsaturated flow the hydraulic conductivity is no longer a constant but varies with changes in water content and indirectly varies with changes in pore-water pressure. The generic 3-D governing equation describing the saturated and unsaturated seepage flow based on mass balance and Darcy law is

$$\frac{\partial}{\partial x} \left(k_x \frac{\partial H}{\partial x} \right) + \frac{\partial}{\partial y} \left(k_y \frac{\partial H}{\partial y} \right) + \frac{\partial}{\partial z} \left(k_z \frac{\partial H}{\partial z} \right) = m_w \gamma_w \frac{\partial H}{\partial t} \tag{3}$$

Where k_x, k_y, k_z are known function of (x, y, z) , the variable H is the total head as a function of space (x, y, z) , m_w is the slope of the storage curve and γ_w is unit weight of water.

Under steady-state conditions, the flux entering and leaving an elemental volume is the same at all times. The right side of the equation consequently vanishes and the equation reduces to

$$\frac{\partial}{\partial x} \left(k_x \frac{\partial H}{\partial x} \right) + \frac{\partial}{\partial y} \left(k_y \frac{\partial H}{\partial y} \right) + \frac{\partial}{\partial z} \left(k_z \frac{\partial H}{\partial z} \right) = 0 \tag{4}$$

The possible boundary conditions are as follows:

- Essential boundary condition: H specified.
- Natural boundary condition-specified normal derivative along a boundary.

$$k \frac{\partial H}{\partial n} \equiv \left(k_x \frac{\partial H}{\partial x} n_x + k_y \frac{\partial H}{\partial y} n_y + k_z \frac{\partial H}{\partial z} n_z \right) = 0 \tag{5}$$

Where n_x, n_y, n_z are the components of the unit normal to the boundary (Bhatti 2005).

3. The research method

3.1 The finite element formulation

The Eq. (4) is a strong form of the boundary value problem that governs the state of the fluid. The semi discrete weak variational formulation of Eq. (4) over V can be expressed by multiplying Eq. (4) at an arbitrary weighting function N_i and applying Green-Gauss theory is given by

$$\iiint_V ([B]^T [C] [B]) dV [H^n] = \iint_A (q [N]^T [N]) dA \quad (6)$$

where

$$[B] = \begin{bmatrix} \frac{\partial N_1}{\partial x} & \frac{\partial N_2}{\partial x} & \dots & \frac{\partial N_n}{\partial x} \\ \frac{\partial N_1}{\partial y} & \frac{\partial N_2}{\partial y} & \dots & \frac{\partial N_n}{\partial y} \\ \frac{\partial N_1}{\partial z} & \frac{\partial N_2}{\partial z} & \dots & \frac{\partial N_n}{\partial z} \end{bmatrix}$$

$[B]$ is gradient matrix with $\frac{\partial N_1}{\partial x}, \frac{\partial N_1}{\partial y}, \frac{\partial N_1}{\partial z}, \dots$ equal to the derivative of the interpolation function with respect to x, y and z that n is the number of junctions in each element

$$[C] = \begin{bmatrix} k_x & 0 & 0 \\ 0 & k_y & 0 \\ 0 & 0 & k_z \end{bmatrix}$$

$[C]$ is element hydraulic conductivity matrix with k_x, k_y, k_z equal to the components of the permeability tensor for the element

$$[H^n] = \begin{bmatrix} H_1 \\ H_2 \\ \vdots \\ H_n \end{bmatrix}$$

$[H^n]$ is vector of nodal heads with H_i equal to the total head at the element nodes

$$[N] = \begin{bmatrix} N_1 \\ N_2 \\ \vdots \\ N_n \end{bmatrix}$$

$[N]$ is vector of interpolating function with N_i equal to the interpolation function over element; q is unit flux across the faces of an element, V and A are the volume and surface of the element, respectively. After Gauss numerical integration, Eq. (6) can be simplified as follows

$$[D] \cdot [H^n] = [F] \quad (7)$$

where

$$[D] = \sum_{j=1}^m [B_j]^T [C] [B_j] \det[J_j] W_j; \quad [J_j] = \begin{bmatrix} \frac{\partial x}{\partial r} & \frac{\partial y}{\partial r} & \frac{\partial z}{\partial r} \\ \frac{\partial x}{\partial s} & \frac{\partial y}{\partial s} & \frac{\partial z}{\partial s} \\ \frac{\partial x}{\partial t} & \frac{\partial y}{\partial t} & \frac{\partial z}{\partial t} \end{bmatrix};$$

$[D]$ is the stiffness matrix, j is integration Gauss point, m is number of integration Gauss points, $[B_j]$ is gradient matrix on Gauss points, $\det[J_j]$ is determinant of the Jacobian matrix, r , s and t rather than x , y and z in master element and $[F]$ is the flux vector reflecting on boundary conditions.

The element matrix for each element in the discretized finite element mesh can be formed and assembled into a global system of simultaneous equations. The finite element solution requires the solving of the system of simultaneous equations. Due to the linearity of the general seepage equation, Gauss elimination method is used to obtain the correct nodal total heads. Secondary quantities, such as pore-water pressure, gradients, velocities, and flux quantities can be calculated based on the nodal total heads. The equation for nodal pore-water pressure

$$[u_w] = ([H^n] - [Z^n]) \gamma_w \quad (8)$$

Where Z^n is elevation at the nodes of the elements. The gradient at each Gauss or integration point is computed from the equation

$$\begin{bmatrix} i_x \\ i_y \\ i_z \end{bmatrix} = [B][H^n] \quad (9)$$

The Darcian velocities at each Gauss point are computed from the equation

$$\begin{bmatrix} v_x \\ v_y \\ v_z \end{bmatrix} = [C][B][H^n] \quad (10)$$

The equation for flux

$$[Q] = [D][H^n] \quad (11)$$

Where $[Q]$ is element flux vector.

3.2 The implemented model, Seep3D

The finite element solution has been implemented into a computer program called, Seep3D. This Software can model both transient and steady state seepage through saturated-unsaturated soil systems. It can apply to complex geometries with arbitrary degrees of heterogeneity and anisotropy. Seep3D model uses a general set of interpolating functions by finite element method with three fundamental solid types for creating of model geometry: hexahedron, tetrahedron and prism region that the global and local coordinate's r , s and t for hex element is shown in Fig. 2.

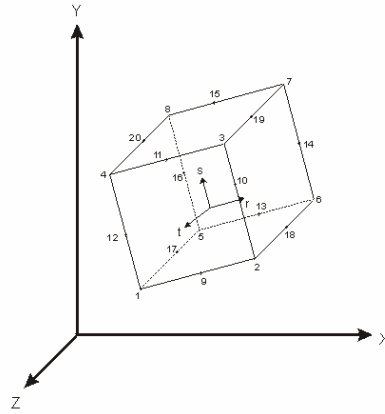


Fig. 2 Global and local coordinate systems of a hex element

A finite element analysis is accomplished in three steps. The first step is to model the problem. This involves designing the finite element mesh, defining the material properties, and specifying the boundary conditions. The second step is to analyze the model formulating and solving the finite element equations. The final step is to view the results through contouring and graphing. For linear analyses when the material properties are constant, the nodal total head can be computed directly. However, in the cases of nonlinear analyses, when the material hydraulic conductivity is a function of total head, the correct material properties are not known at the start of the analysis. Consequently, an iterative scheme is required to solve the equations.

3.3 Neural network model

For the artificial neural network modeling, measured data sets are used to train and test the developed model. In this study, measured data sets used during modeling include water levels in the piezometers and the water levels on the upstream and downstream sides of body dam by the Monitoring Center of dam. The model is a four-layer feedforward artificial neural network, as shown in Fig. 3. The ANN feedforward model is employed a sigmoid function as activator and a back-propagation algorithm for network learning that the input quantities (x_i) are multiplied in connection weights (w_{ij}) and summation with a bias. Then, the results are moved into the input layer neurons and they pass to the hidden layer neurons (y_i).

$$net_j = \sum x_i w_{ij} + b_j \quad (12)$$

After creating of net_j , the result passes on through a generally employed nonlinear sigmoid transfer function.

$$f(net_j) = \frac{1}{1 + e^{-net_j}} \quad (13)$$

The objective of the back-propagation algorithm is to find the optimal weights that would generate an output vector $y = (y_1, y_2, \dots, y_p)$ as close to the target values of the output vector $T = (t_1, t_2, \dots, t_p)$ as possible with the selected accuracy. The optimal weights are found by minimizing a predetermined error function (E) of the following form

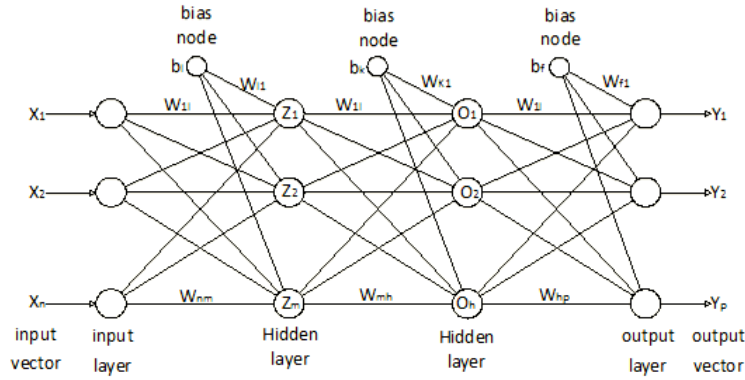


Fig. 3 Layout of four layer feed-forward artificial neural network

$$E = \sum_{i=1}^p (y_i - t_i)^2 \tag{14}$$

Where y_i and t_i are components of ANN output vector Y and target output vector T ; p is number of output neurons. In the back-propagation algorithm, the effect of the input is first passed forward through the network to reach the output layer. After the error is computed, it is then propagated back towards the input layer with the weights being modified. The gradient descent method, along with the chain rule of differentiation, was employed to modify the network weights as

$$\Delta w_{ij}(n) = -\delta \frac{\partial E}{\partial w_{ij}} + \alpha_m \Delta w_{ij}(n - 1) \tag{15}$$

Where Δw_{ij} and $\Delta w_{ij}(n - 1)$ are weight increments between node i and j during the n th and $(n - 1)$ th pass or epoch; δ is learning rate; and α_m is momentum factor.

An equation similar to Eq. (15) was also used to correct the bias values. The learning rate δ was used to increase the likelihood of avoiding the training process being trapped in a local minimum instead of a global minimum. However, it is possible that the training process can still be trapped in a local minimum despite the use of a learning rate. The solution often follows a zigzag path while trying to reach a minimum error and this may slow down the training process. The momentum factor α_m can be employed to speed up training in very flat regions of the error surface and help prevent oscillations in the weights.

In order to objectively evaluate the model performance, the most commonly employed error measures, such as the root mean square error (RMSE) and the mean absolute error (MAE) were computed for each case. The RMSE and MAE can be defined as (Dolling and Varas 2002)

$$RMSE = \sqrt{\frac{\sum_i^N (W_{mi} - W_{pi})^2}{N}} \tag{16}$$

$$MAE = \frac{\sum_i^N |W_{mi} - W_{pi}|}{N} \tag{17}$$

Where W_m and W_p are the measured water level and the predicted water level; N is the number of observations.

In addition to this, different scenarios were modeled by utilizing different layers, activation functions and different inputs. The correlation coefficient R^2 is important because it measures if the fit is good. If the value of it is close to 1, the slope of the regression line is almost one and the intercept is close to zero.

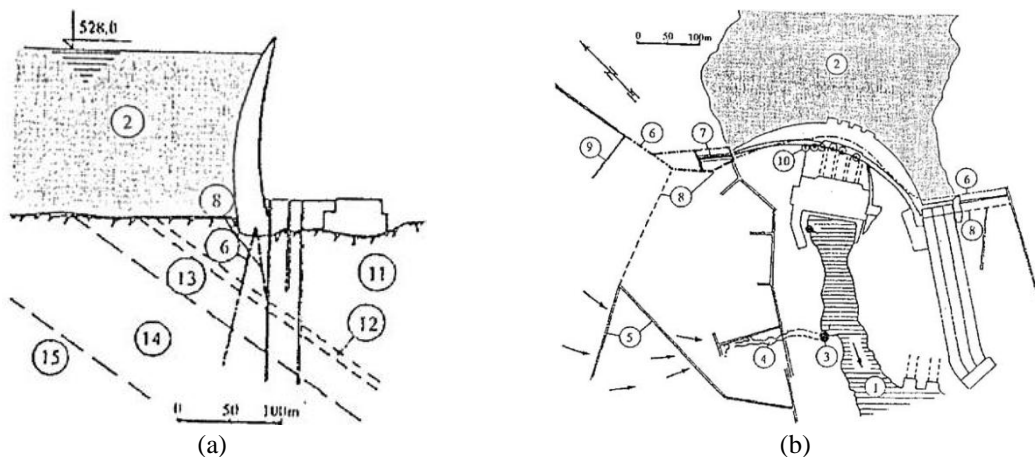
4. Application of model to the Shahid Abbaspour Dam

The Shahid Abbaspour Dam is located in the Khuzestan province at southwestern of Iran, at 52km northeast of the Masjid-I-solaiman city. This dam controls and regulates water flow of the biggest river in Iran. This is a multipurpose dam to supply water for 132000 ha agricultural lands, generating energy (1000 mega Watt) and controlling flood flow of Karun River. Fig. 4 indicates general layout of the Shahid Abbaspour Dam.

The Shahid Abbaspour Dam with 380 m length and 200 m high located at 542 m above sea level. Fig. 5 shows position of piezometers in dam foundation.

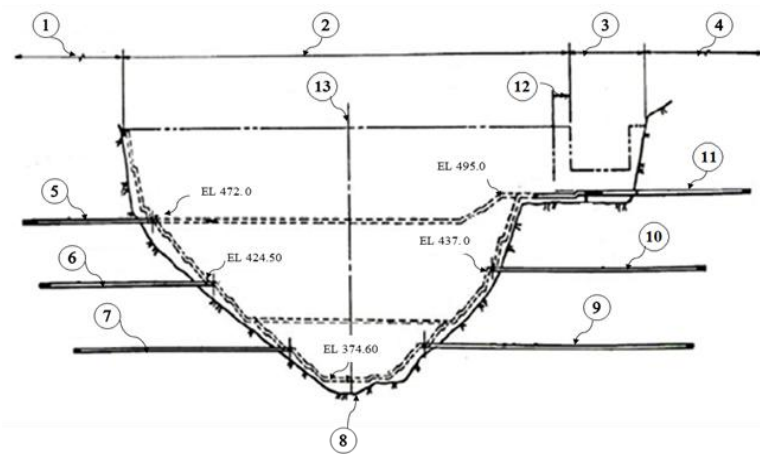
The dam is located on the great anticline domain of Asmara limestone. In foundation, a thick clay layer is impervious by concrete injection.

The seepage flow is affected by the pressure gradient due to the difference in the water levels at the upstream and downstream sides of the dam and drainages. The piezometers are located in dam foundation in order to monitoring of flow (See Figs. 5-6). The five piezometers which were located at the dam foundation (labeled as 8D₁, 9D₃, 10D₃, 13D₄ and 15D₁) were chosen and the water levels at the piezometers have been measured every 1 or 2 weeks. The measured water levels at the piezometers at the upstream and downstream of dam for the period of January 29, 1992 to July 17, 2002 are presented in Fig. 7.



1. Karun River; 2. Reservoir; 3. Big Spring; 4. Big Spring karst channel; 5. Gallery;
6. Grout curtain; 7. Cutoff; 8. Drainage curtain; 9. fan grout curtain; 10. Relief wells;
11. Middle Asmari limestone; 12. Impervious shale zone; 13. Principal vuggy zone;
14. Lower Asmari limestone; 15. Eocene shale (Ghobadi *et al.* 2005)

Fig. 4 General layout of the Shahid Abbaspour Dam site



1. Right abutment; 2. Arch dam; 3. Spillway; 4. Left abutment; 5. RDA₃; 6. RDA₂; 7. RDA₁; 8. Foundation Gallery (8D1-15D1); 9. LDA₁; 10. LDA₂; 11. LDA₃; 12. Thrust block; 13. Line of arch center

Fig. 5 Layout of body and abutment the Shahid Abbaspour Dam

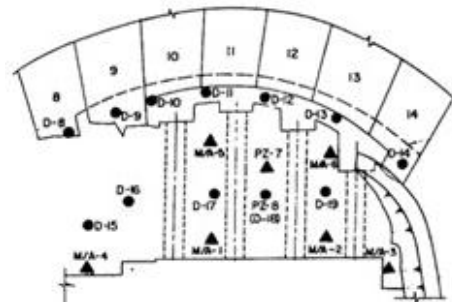


Fig. 6 Position of piezometers at dam foundation

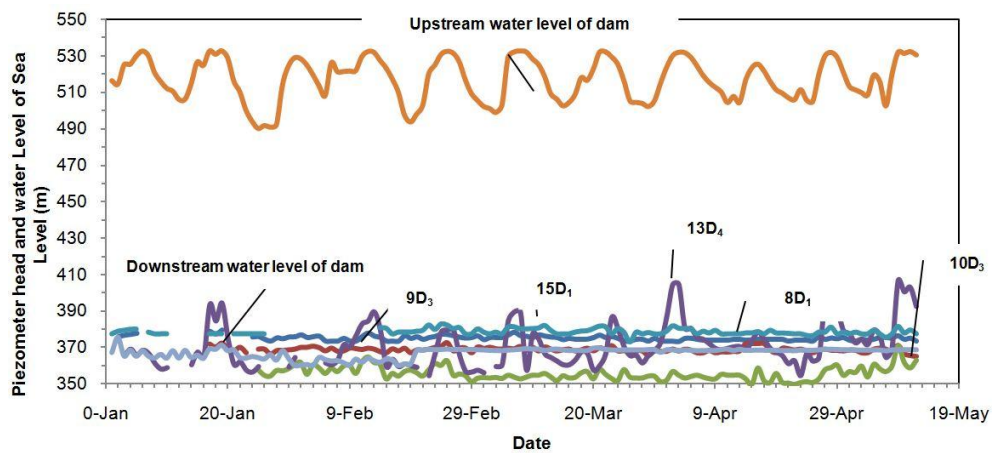


Fig. 7 Temporal variations of piezometer heads at the upstream and downstream of dam

According to the observed records, the maximum water levels at the upstream and downstream of dam for this period are equal to 532.51 and 370.15 m from sea level, respectively.

5. Boundary conditions

The numerical solution of Eq. (11) requires suitable specification of boundary conditions. The soil-water pressure field in domain of numerical modeling needs to be specified. For the boundary conditions, as appropriate, the Neumann and Dirichlet conditions can be specified. As for as the dam body is concrete, it was assumed that the dam body was completely tight and impermeable and the Neumann boundary condition of zero water flux was employed for this segment of the boundary. The Dirichlet boundary conditions in terms of the water level on the upstream and downstream sides of the reservoir were expressed at the left and right parts of the analyzed cross section. In the drainage gallery, the Dirichlet boundary condition was employed as $H_0 = z + h_0$ for Drains D-8 to D-14. The impermeable boundary of the lower layer was described by the Neumann boundary condition, i.e., $q = 0.0$ (lower part of Eocene shale-See Fig. 4).

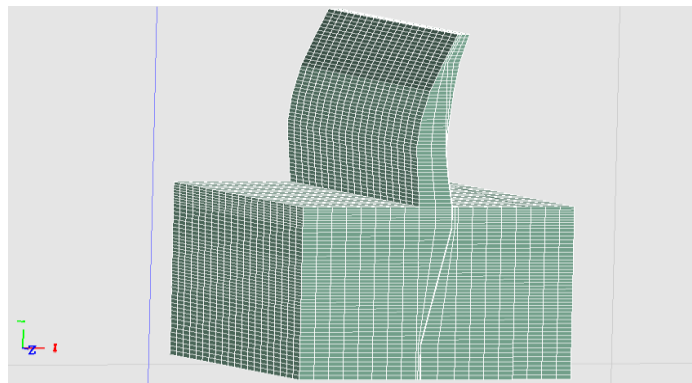


Fig. 8 Layout of meshing the computational network of finite element model (Seep3D)

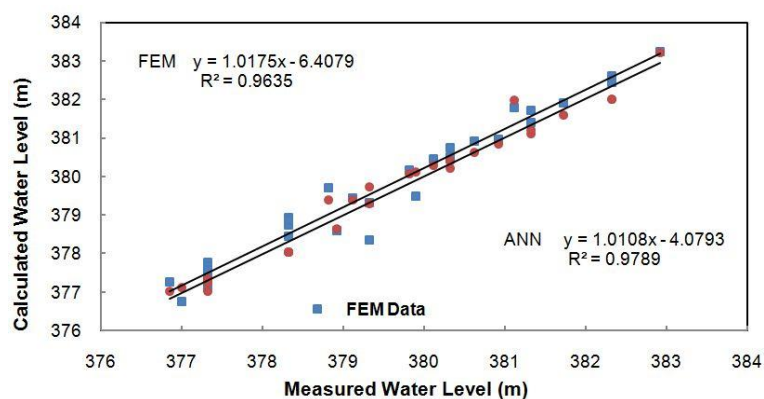
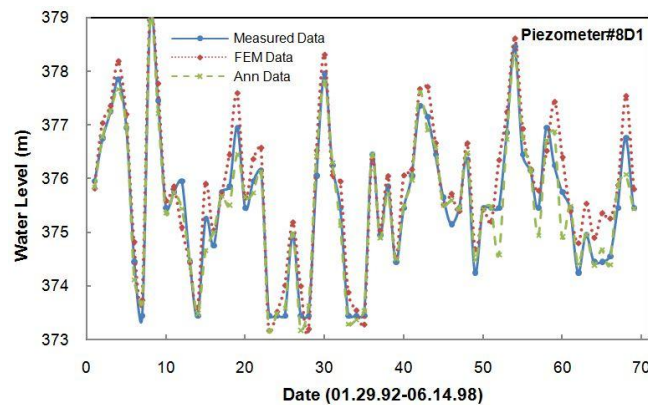


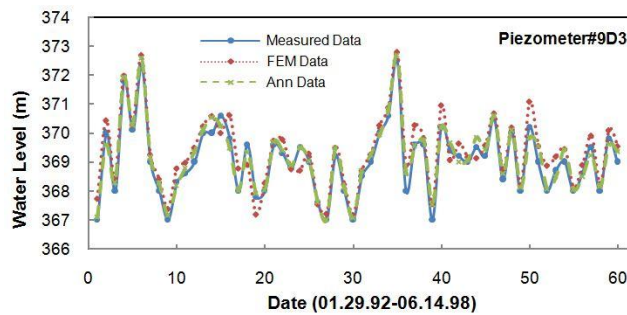
Fig. 9 Measured water levels versus predicted water levels by FEM and ANN models at the calibration stage for piezometer 15D₁

6. Results and discussion

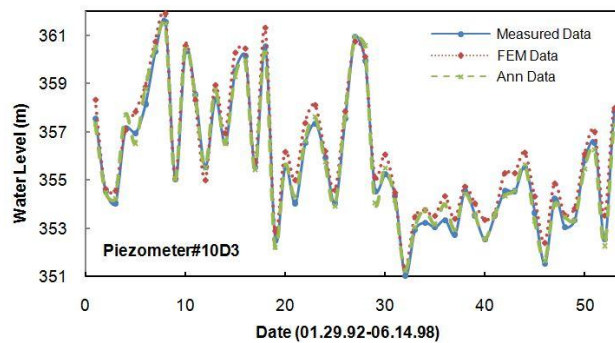
The region of interest (cross section of Shahid Abbaspour Dam) was divided into hexahedron finite elements, as shown in Fig. 8. The network was composed of 24960 hexahedron elements and 28707 nodal points; it was made denser in the dam foundation and in the neighborhood of the curtain screen (Fig. 8). The data obtained from piezometers 8D₁, 9D₃, 10D₃, 13D₄ and 15D₁, as shown in Fig. 7, were used for model calibration and verification.



(a)

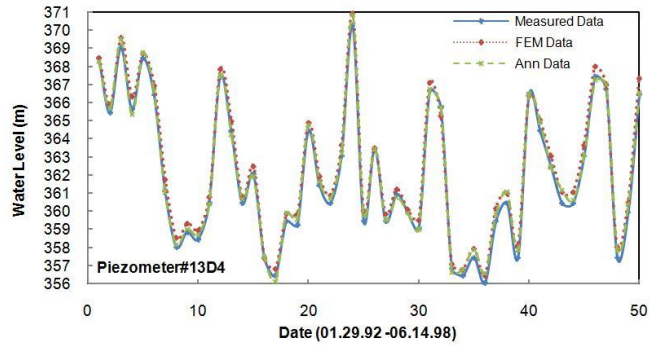


(b)

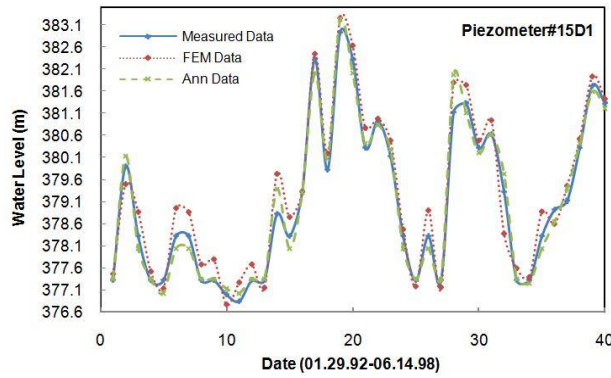


(c)

Fig. 10 Calculated and measured water levels at piezometer (a)8D₁, (b)9D₃, (c)10D₃, (d)13D₄, (e)15D₁ for the period from Jan 29, 1992 to Jun 14,1998. Calibration run



(d)



(e)

Fig. 10 Continued

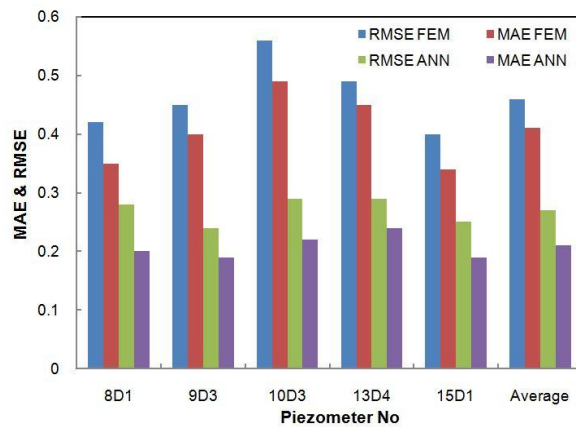


Fig. 11 Calculated error-calibration run

The model was calibrated by comparing the model results with the measured data from Jan 29, 1992 to Jun 14, 1998. Fig. 9 presents the calibration runs comparing the predicted model results with the measured water level values of each piezometer.

The model-predicted water level for each piezometer is given in Fig. 10 from which it is seen that the ANN model satisfactorily predicted the measured water level in each piezometer.

The calculated RMSE and MAE values for calibration run as shown in Fig. 11.

Using the measured data for the period of July 15, 1998 to July 17, 2002, the model was validated and its prediction results were compared with the measured data as shown in Fig. 13.

The Fig. 12 presents the validation runs comparing the predicted model results with the

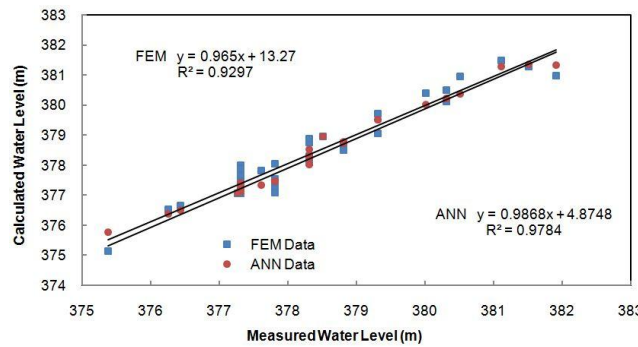
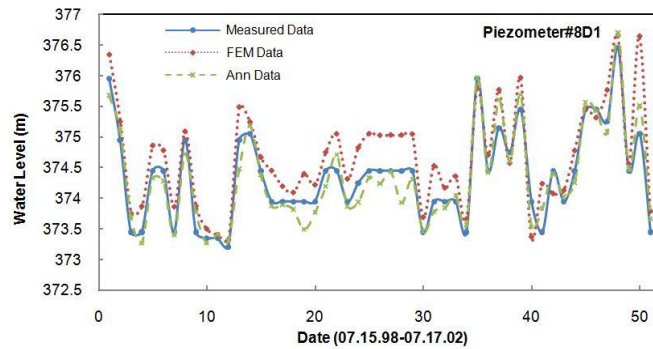
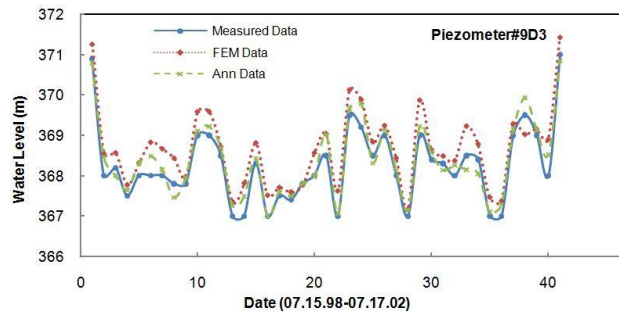


Fig. 12 Measured water levels versus predicted water levels by FEM and ANN models at the validation stage for piezometer 15D₁

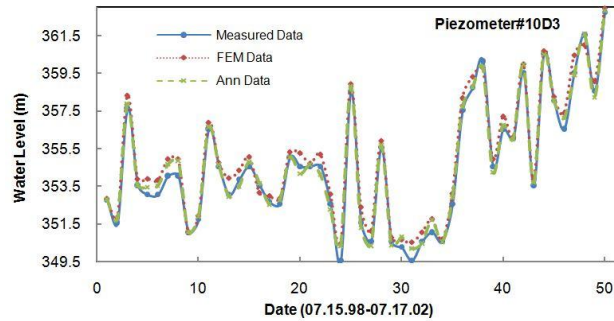


(a)

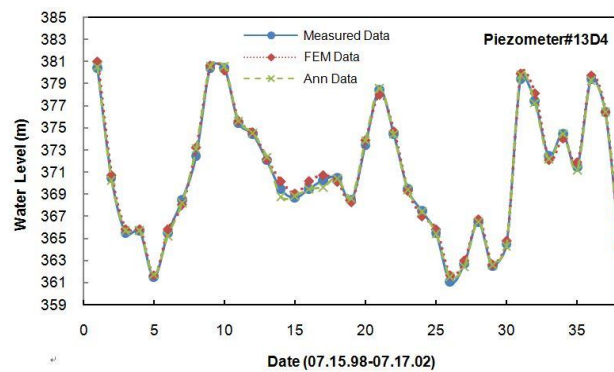


(b)

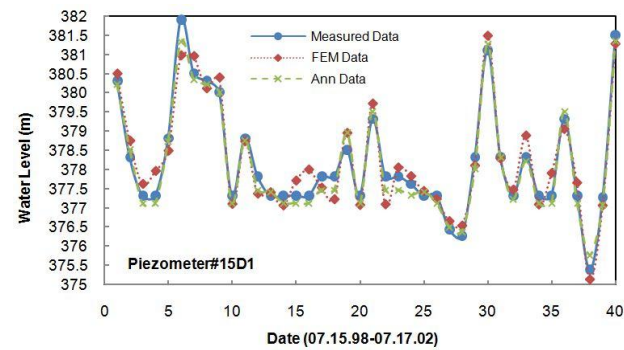
Fig. 13 Calculated and measured water levels at piezometer (a)8D₁, (b)9D₃, (c)10D₃, (d)13D₄, (e)15D₁ for the period from Jul 15, 1998 to Jul 17,2002. Validation run



(c)



(d)



(e)

Fig. 13 Continued

measured water level of piezometer 15D₁. Also, the calculated RMSE and MAE values for validation run as shown in Fig. 14.

In order to obtain the reliability and accuracy of the FEM model, the sequence of meshes were used for modeling of dam foundation. The meshes consist of coarse, medium and fine meshes by 5433, 7692, 10583, 13440, 17280 and 24960 elements for FEM model, respectively. Also, we defined the relative error as the error normalized by the corresponding value of the numerical solution. The Convergence results for the relative error are shown in Fig. 15.

When the ANN model is compared with the FEM as in Fig. 10 and 13, it is seen that the ANN

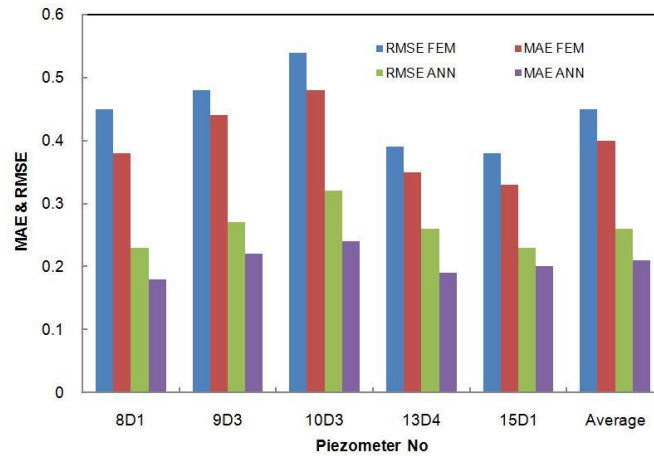


Fig. 14 Calculated error-validation run

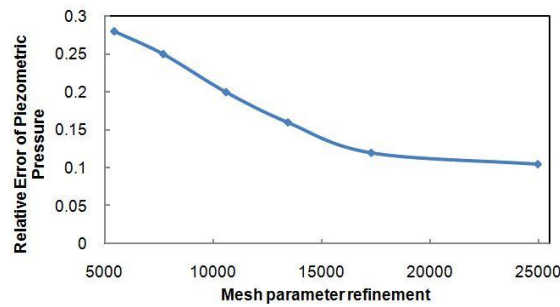


Fig. 15 Convergence of the relative error of piezometric pressure for FEM discretization

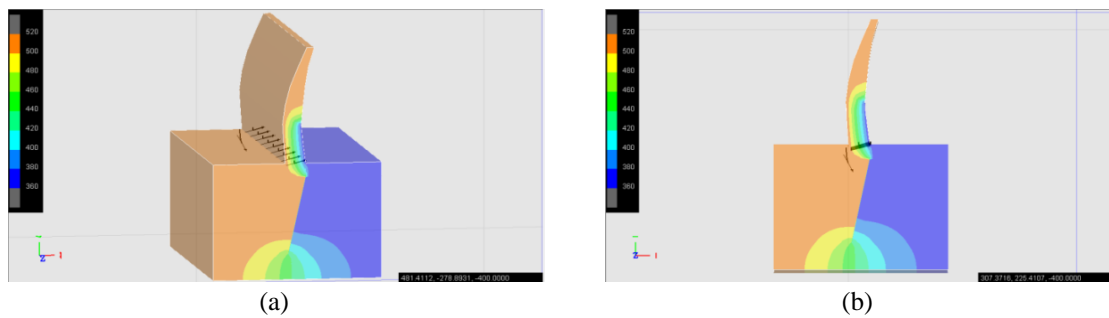


Fig. 16 The graphical results of total head in FEM model

model is as good as the FEM, especially for piezometers 15D₁. In the case of predicting the water level in 15D₁, the ANN model performed better than the FEM as seen in Figs. 9 and 12. The physics-based of FEM represents our best understanding of the physical process. In this model, the relations among the input and output variables are well-defined. Therefore it has universal applicability. Using this model, it is possible to obtain spatial and temporal variations of the state variables over the domain of interest under different values of the model parameters. Such

information might be essential, especially for investigating any undesired cases that might happen and be detrimental to dam safety. The Fig. 16 presents the graphical results of FEM for the Shahid Abbaspour Dam.

7. Conclusions

This study provides finite element and ANN models to predict piezometric head and seepage through the foundation of a concrete dam. In order to investigate of correct performance, both models were applied to predict temporal and spatial variation of flow through the Shahid Abbaspour Dam in Iran. Both models were calibrated and verified using the 30-year measured data of the piezometers placed on foundation dam for monitoring seepage. The suitable prediction in time and space of the seepage path through the foundation dam by the models indicates that these models can be employed to verify the piezometer readings to detect the unusual in the meanwhile of pore water and seepage and hence these models can be used in planning and implemental works and economically suitable for stability measures.

The results of this study have been exhibited that the FEM and ANN models are capable of simulating the seepage problem. The structure of ANN model is simple which has ability to learn from datum without the need of explicit physics and it can models temporal variations of variables, whereas the FEM yields spatial and temporal variations of variables. The results of ANN model are more exact in compare with FEM and the correlation coefficient R^2 is higher at the most of piezometers in the calibration and validation stage. The FEM presents the graphical results of problem solving therefore the seepage path can be easily traced and it is useful to planning and dam safety. At last, both FEM and ANN models produce results that are in excellent agreement with those obtained at complicated solutions.

References

- Arun, K.J. and Reddi, L.N. (2011), "Finite-depth seepage below flat aprons with equal end cutoffs", *J. Hydraul. Eng.*, **137**(12), 1659-1667.
- ASCE Task Committee (2000), "Artificial neural networks in hydrology, II: Hydrologic applications", *J. Hydrol. Eng.*, **5**(2), 124-137.
- Ataie-Ashtiani, B., Volker, R.E. and Lockington, D.A. (1999), "Numerical and experimental study of seepage in unconfined aquifers with a periodic boundary condition", *J. Hydrol.*, **222**(1-4), 165-174.
- Ayoubloo, M.K., Azamathulla, H.Md., Jabbari, E. and Mahjoobi, J. (2011), "Model tree approach for estimation of critical submergence for horizontal intakes in open channel flows", *Expert Syst. Appl.*, **38**(8), 10114-10123.
- Aziz, A.R.A. and Wong, K.V. (1992), "A neural-network approach to the determination of aquifer parameters", *J. Ground Water*, **30**(2), 164-166.
- Azamathulla, H.Md., Deo, M.C. and Deolalikar, P.B. (2005), "Neural networks for estimation of scour downstream of ski-jump bucket", *J. Hydraul. Eng.*, **131**(10), 898-908.
- Azamathulla, H.Md., Deo, M.C. and Deolalikar, P.B. (2006), "Estimation of scour below spillways using neural networks", *IAHR, J. Hydraul. Res.*, **44**(1), 61-69.
- Azamathulla, H.Md., Deo, M.C. and Deolalikar, P.B. (2008), "Alternative neural networks to estimate the scour below spillways", *Adv. Eng. Software*, **39**(8), 689-698.
- Azamathulla, H.Md. and Zakaria, N.A. (2011), "Prediction of scour below submerged pipeline crossing a river using ANN", *IWA - Water Sci. Technol.*, **63**(10), 2225-2230.
- Bhatti, M.A. (2005), *Fundamental Finite Element Analysis and Applications With Mathematica and Matlab*

- Computations*, John Wiley & Sons Inc., Hoboken, NJ, USA.
- Caudill, M. and Butler, C. (Eds.) (1987), *IEEE First International Conference on Neural Networks*, San Diego, CA, USA.
- Chang, Y.Ch., Chen, G.Y. and Yeh, H.D. (2010), "Transient flow into a partially penetrating well during the constant-head test in unconfined aquifers", *J. Hydraul. Eng.*, **137**(9), 1054-1064.
- Childs, E.C. and Collins-George, N. (1950), "The permeability of porous materials", *Proc. R. Soc. London*, **201**(A), 392-405.
- Cooley, R.L. (1971), "A finite difference method for unsteady flow in variably saturated porous media: application to a single pumping well", *Water Resour. Res.*, **7**(6), 1607-1625.
- Dolling, O.R. and Varas, E.A. (2002), "Artificial neural networks for streamflow prediction", *J. Hydraul. Res.*, **40**(5), 547-554.
- Fredlund, D.G. and Rahardjo, H. (1993), *Soil Mechanics for Unsaturated Soils*, Wiley, Chichester, pp. 136-140.
- Geo-Slope International (2001), *Seep3D Software (Version 1)*, Calgary, AL, Canada.
- Ghobadi, M.H., Khanlari, G.R. and Djalaly, H. (2005), "Seepage problems in the right abutment of the Shahid Abbaspour", *Eng. Geol.*, **82**(2), 119-126.
- Honjo, Y., Giao, P.H. and Naushahi, P.A. (1995), "Seepage analysis of Tarbela dam (Pakistan) using finite element method", *Int. J. Rock Mech. Min. Sci. Geomech. Abstr.*, **32**(3), 131A.
- Jain, A. and Reddi, L. (2011), "Finite-depth seepage below flat aprons with equal end cutoffs", *J. Hydraul. Eng.*, **137**(6), 1659-1668.
- Jain, S.K. (2001), "Development of integrated sediment rating curves using ANNs", *J. Hydraul. Eng.*, **127**(1), 30-37.
- Krikland, M.R., Hills, R.G. and Wierenga, P.J. (1992), "Algorithms for solving Richard's equation for variably saturated soils", *Water Resour. Res.*, **28**(8), 2049-2058.
- Li, L., Barry, D.A. and Pattiaratchi, C.B. (1997), "Numerical modeling of tidal-induced beach water table fluctuations", *Coast. Eng.*, **30**(1-2), 105-123.
- Money, R.L. (2006), "Comparison of 2D and 3D Seepage model results for excavation near levee toe", *GeoCongress*, Atlanta, GA, USA, pp. 1-4.
- Nagy, H.M., Watanabe, K. and Hirano, M. (2002), "Prediction of sediment load concentration in rivers using artificial neural network model", *J. Hydraul. Eng.*, **128**(6), 588-595.
- Panthulu, T.V., Krishnaiah, C. and Shirke, J.M. (2001), "Detection of seepage paths in earth dams using self-potential and electrical resistivity methods", *Eng. Geol.*, **59**(3-4), 281-295.
- Rajurkar, M.P., Kothiyari, U.C. and Chaube, U.C. (2002), "Artificial neural networks for daily rainfall-runoff modeling", *Hydrol. Sci. J.*, **47**(6), 865-878.
- Rajurkar, M.P., Kothiyari, U.C. and Chaube, U.C. (2004), "Modeling of daily rainfall-runoff relationship with artificial neural network", *J. Hydrol.*, **285**(1-4), 96-113.
- Rubin, J. (1968), "Theoretical analysis of two-dimensional, transient flow of water in unsaturated and partly saturated soils", *Soil Sci. Soc. Am. Proc.*, **32**(5), 607-615.
- Tayfur, G. (2002), "Artificial neural networks for sheet sediment transport", *Hydrol. Sci. J.*, **47**(6), 879-892.
- Tayfur, G., Swiatek, D., Wita, A. and Singh, V.P. (2005), "Case study: Finite element method and artificial neural network models for flow through Jeziorsko Earthfill Dam in Poland", *J. Hydrol.*, **131**(6), 431-440.
- Tien-Kuen, H. (1996), "Stability analysis of an earth dam under steady state seepage", *Comput. Struct.*, **58**(6), 1075-1082.
- Tokar, A.S. and Johnson, P.A. (1999), "Rainfall-runoff modeling using artificial neural networks", *J. Hydrol. Eng.*, **4**(3), 232-239.
- Turkmen, S., Ozguler, E., Taga, H. and Karaogullarindan, T. (2002), "Seepage problems in the karstic limestone foundation of the Kalecik Dam (South Turkey)", *Eng. Geol.*, **63**(3-4), 247-257.
- Xu, Y.Q., Unami, K. and Kawachi, T. (2003) "Optimal hydraulic design of earth dam cross section using saturated-unsaturated seepage flow model", *Adv. Water Resour.*, **26**(1), 1-7.